10

Fixed-Node Approximation

10.1 The Sign Problem

In the previous Chapters, we have discussed two approaches that can be used to sample the exact ground-state wave function of a correlated many-body problem. Both of them are based upon the projection technique, in which the ground state is filtered out from an initial trial state; for example, within the Green's function Monte Carlo technique, we have that:

$$\lim_{n\to\infty} (\Lambda - \mathcal{H})^n |\Psi_0\rangle \approx (\lambda - E_0)^n |\Upsilon_0\rangle, \tag{10.1}$$

where Λ is a diagonal operator, with $\Lambda_{x,x} = \lambda$ being a sufficiently large constant, and E_0 is the ground-state energy. Here, the only assumption is that the initial state $|\Psi_0\rangle$ must have a finite overlap with the ground state $|\Upsilon_0\rangle$. Within the stochastic implementation of the power method, it is necessary that the so-called Green's function $\mathcal{G}_{x',x}$ defined in Eq. (8.5) is *non negative* for *all* the elements of the basis set $\{|x\rangle\}$. In some cases, negative terms can be changed into positive ones by including importance sampling; this approach leads to the modified Green's function given in Eq. (8.31). However, in the generic case, the importance sampling cannot remove all the negative elements and we have to face the so-called *sign problem*. In turn, the signs of the Green's function induce the sign structure of the ground-state wave function:

$$|\Upsilon_0\rangle = \sum_x \Upsilon_0(x)|x\rangle, \tag{10.2}$$

where $\Upsilon_0(x) = \langle x|\Upsilon_0\rangle$ can be either positive or negative and its sign is usually *a priori* unknown. Of course, when $\mathcal{G}_{x,x'} \geq 0$, corresponding to a Hamiltonian with all non-positive off-diagonal elements $\mathcal{H}_{x,x'}$, the ground-state wave function has $\Upsilon_0(x) \geq 0$; the strict positivity of the amplitudes can be demonstrated by using the Perron-Frobenius theorem (Meyer, 2000).

https://doi.org/10.1017/9781316417041.011 Published online by Cambridge University Press

Here, we would like to discuss the main issues related to the presence of negative elements in the Green's function and one possible remedy to it, namely the *fixed-node* approximation. In the following, we will limit ourself to *real* wave functions (corresponding to Hamiltonians with real matrix elements), a case that is already tremendously complicated. First of all, we emphasize that the sign problem is *basis dependent*: while the Green's function may have negative entries in a given basis $\{|x\rangle\}$, it may have all positive entries in another basis $\{|y\rangle\}$. Notice that the diagonal elements are not relevant, since they can be made always positive by a suitable shift of $\Lambda_{x,x} = \lambda$. Therefore, the straightforward solution of the sign problem is to choose a clever basis set, such that $\mathcal{G}_{x,x'} \geq 0$ for all the matrix elements. Unfortunately, this possibility can be obtained only in very limited cases. Indeed, for computational reasons of efficiency, the most commonly used basis sets are local ones, which are defined on each individual site or, at most, involve few neighboring sites. In the general case, local basis sets lead to a severe sign problem. Instead, the sign problem would be absent in the basis set that diagonalizes the Hamiltonian; unfortunately, this basis cannot be determined in a reasonable computing time.

In principle the stochastic implementation of the projection scheme can be generalized to the cases where the Green's function has negative entries, by associating the sign to the weight of the walker. In particular, we can consider the following decomposition of the Green's function (here, to simplify the notation, we do not put a tilde over the various quantities, assuming that importance sampling is considered):

$$\mathcal{G}_{x',x} = |\mathcal{G}_{x',x}| s_{x',x} = p_{x',x} b_x s_{x',x}, \tag{10.3}$$

where, similarly to Eq. (8.7), we have defined a transition probability $p_{x',x}$, a weight b_x, and also a sign $s_{x',x}$ as:

$$b_x = \sum_{x'} |\mathcal{G}_{x',x}|, \tag{10.4}$$

$$p_{x',x} = \frac{|\mathcal{G}_{x',x}|}{b_x}, \tag{10.5}$$

$$s_{x',x} = \text{sign}(\mathcal{G}_{x',x}). \tag{10.6}$$

Then, a Markov process can be implemented, generalizing the one used within the Green's function Monte Carlo, see Eqs. (8.10) and (8.11):

$$\text{1) generate } x_{n+1} = x' \text{ with probability } p_{x',x_n}, \tag{10.7}$$

$$\text{2) update the weight with } w_{n+1} = w_n b_x, \tag{10.8}$$

$$\text{3) attach the sign to the weight } w_{n+1} = w_{n+1} s_{x_{n+1},x_n}. \tag{10.9}$$

This approach can be generalized to N_w walkers, as discussed in section 8.5; the branching procedure can be performed according to the absolute value of

https://doi.org/10.1017/9781316417041.011 Published online by Cambridge University Press

the weights $|w_{\alpha,n}|$, with $\alpha = 1, \ldots, N_{\rm w}$. In this way, walkers will be distributed according to the distribution probability $\mathcal{P}_n^F(x,w)$, where now the important difference with what has been discussed in Chapter 8 is that $\mathcal{P}_n^F(x,w) \neq 0$ also for $w < 0$. Then, in analogy with Eq. (8.16), the fermionic wave function is given by:

$$\Psi_n^F(x) \equiv \int dw\ w\ \mathcal{P}_n^F(x,w). \tag{10.10}$$

The fermionic properties are encoded in the presence of non-trivial signs, i.e., within a small asymmetry of the distribution function:

$$\mathcal{P}_n^F(x,w) \neq \mathcal{P}_n^F(x,-w). \tag{10.11}$$

Instead, by disregarding the signs, i.e., by eliminating the third step of Eq. (10.9), the Markov process converges to the "bosonic" ground state given by the lowest-energy state of the Hamiltonian $\mathcal{H}^B_{x,x'} = -|\mathcal{H}_{x,x'}|$ for $x \neq x'$ and $\mathcal{H}^B_{x,x} = \mathcal{H}_{x,x}$. In this case, the walkers will have a non-vanishing probability only for $w > 0$ and the ground-state wave function will be given by:

$$\Psi_n^B(x) \equiv \int dw\ |w|\ \mathcal{P}_n^F(x,w). \tag{10.12}$$

The crucial point is that the fermionic character can be hardly detected in Monte Carlo simulations. Indeed, let us consider a generic observable $\mathcal{O}$ and take the mixed average [see Eq. (8.53)] with $|\Psi_G\rangle = \sum_x |x\rangle$:

$$\frac{\langle \Psi_G|\mathcal{O}|\Psi_n^F\rangle}{\langle \Psi_G|\Psi_n^F\rangle} = \frac{\sum_x \int dw\ w\mathcal{P}_n^F(x,w)\mathcal{O}(x)}{\sum_x \int dw\ w\mathcal{P}_n^F(x,w)}, \tag{10.13}$$

where $\mathcal{O}(x) = \sum_{x'} \mathcal{O}_{x',x}$. Then, by using the reweighting technique described in section 3.2 and denoting the sign of the weight w by $s(w)$, we get:

$$\frac{\sum_x \int dw\ w\mathcal{P}_n^F(x,w)\mathcal{O}(x)}{\sum_x \int dw\ w\mathcal{P}_n^F(x,w)} = \frac{\dfrac{\sum_x \int dw\ |w|s(w)\mathcal{P}_n^F(x,w)\mathcal{O}(x)}{\sum_x \int dw\ |w|\mathcal{P}_n^F(x,w)}}{\dfrac{\sum_x \int dw\ |w|s(w)\mathcal{P}_n^F(x,w)}{\sum_x \int dw\ |w|\mathcal{P}_n^F(x,w)}}. \tag{10.14}$$

Therefore, the previous fermionic quantity can be obtained by sampling over the "bosonic" probability $|w|\mathcal{P}_n^F(x,w)$:

$$\frac{\sum_x \int dw\ w\mathcal{P}_n^F(x,w)\mathcal{O}(x)}{\sum_x \int dw\ w\mathcal{P}_n^F(x,w)} \approx \frac{\langle\langle s\ \mathcal{O}\rangle\rangle_B}{\langle\langle s\rangle\rangle_B}, \tag{10.15}$$

where $\langle\langle \ldots \rangle\rangle_B$ denotes the statistical average over the probability distribution $|w|\mathcal{P}_n^F(x,w)$. In the general case, almost half of the walker's population will have a positive sign, while the other half population will have a negative sign; this

https://doi.org/10.1017/9781316417041.011 Published online by Cambridge University Press

fact leads to an almost exact cancellation of both numerator and denominator of Eq. (10.15). Indeed, from Eq. (10.1), we have that:

$$\Psi_n^F(x) \approx (\lambda - E_0^F)^n \Upsilon_0^F(x) \approx e^{-nE_0^F} \Upsilon_0^F(x), \tag{10.16}$$

$$\Psi_n^B(x) \approx (\lambda - E_0^B)^n \Upsilon_0^B(x) \approx e^{-nE_0^B} \Upsilon_0^B(x), \tag{10.17}$$

where E_0^F and E_0^B are the ground-state energies of the "fermionic" (i.e., described by $\mathcal{H}$) and "bosonic" (i.e., described by $-|\mathcal{H}|$) systems. Since the "bosonic" ground-state energy is usually much lower than the "fermionic" one, the average sign goes to zero exponentially with the number of particles N_p (both E_0^F and E_0^B being proportional to N_p):

$$\langle\langle s \rangle\rangle_B = \frac{\sum_x \int dw\ |w| s(w) \mathcal{P}_n^F(x,w)}{\sum_x \int dw\ |w| \mathcal{P}_n^F(x,w)} \approx \exp\left[n\left(E_0^B - E_0^F\right)\right] \approx 0. \tag{10.18}$$

Similarly, also $\langle\langle s\ \mathcal{O} \rangle\rangle_B \approx 0$. In particular, in any numerical evaluation of these quantities that is based upon Monte Carlo sampling, the errorbars will become much larger than the value of the observable making prohibitive its estimation (Ceperley and Alder, 1980; Loh et al., 1990).

Historically, the sign problem first appeared in fermionic models on the continuum, for this reason it is also usually called "fermionic sign problem," which is related to the fact that the fermionic wave function is anti-symmetric when interchanging two particles. Therefore, a fermionic wave function cannot be interpreted as a probability density.

On the continuum, a particularly important concept is given by the *nodal surface*, namely the location of the points where $\Upsilon_0(x) = 0$, which separates the regions with opposite signs. In a d-dimensional system with N_p particles, the dimension of the whole phase space is dN_p. Obviously, the dimension of the nodal surface is $dN_p - 1$; instead, the locus of the points where a fermionic wave function vanishes because of the Pauli principle (i.e., whenever the coordinates of two particles coincide) generates a set of surfaces of dimension $dN_p - d$ (denoted as "Pauli surface"). Therefore, the location of the nodes due to the anti-symmetry does not exhaust the nodal surface, except for $d = 1$, but builds its "skeleton." In order to exemplify this concept, we show in Fig. 10.1 the case with $N_p = 49$ free spinless fermions in a two-dimensional box with side $L = 10$ and periodic-boundary conditions; here, we fixed the coordinates of all particles except one and computed the signs of the many-body wave function (a Slater determinant constructed by filling the lowest-energy one-body states, i.e., plane waves) when displacing the last particle in the box (Ceperley, 1991). Remarkably, in one spatial dimension, the Pauli surface alone completely determines the nodal surface, apart from further accidental nodes that may be caused by degeneracies or singular interactions.

https://doi.org/10.1017/9781316417041.011 Published online by Cambridge University Press

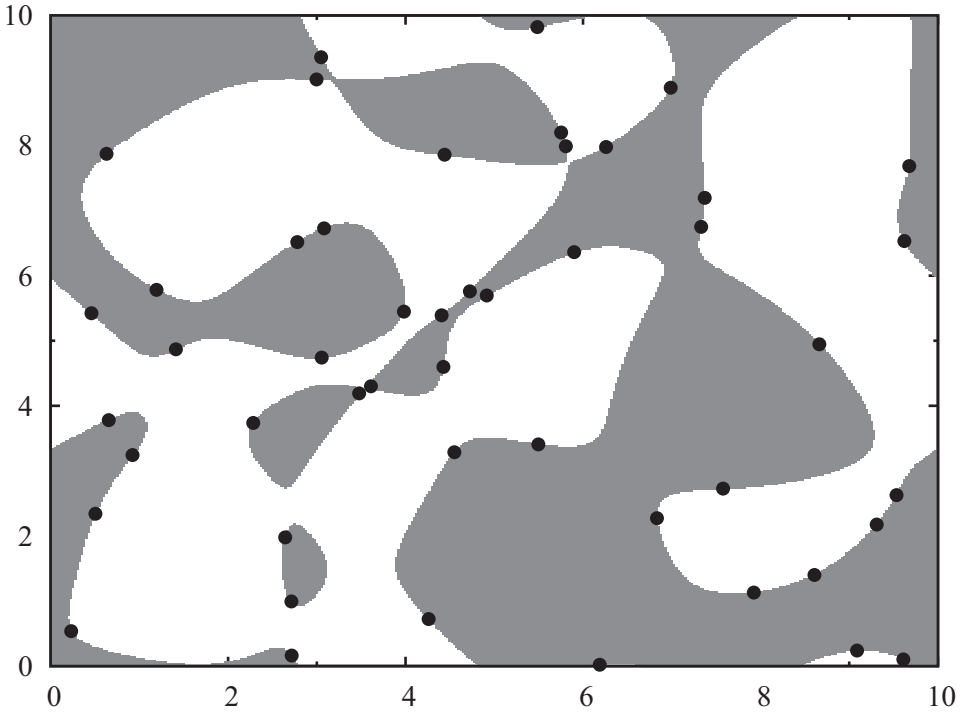

Figure 10.1 The nodal and Pauli surfaces are shown for a system of 49 free spinless fermions in a two-dimensional box of side $L = 10$ with periodic boundary conditions. The coordinates of 48 particles are fixed (randomly) in the box and denoted by black dots. The last particle is displaced in the box and the signs of the many-body wave function are computed. The Pauli surface (or better, its projection in the subspace with the 48 particles frozen in the box) coincides with the black dots. The many-body wave function is positive (negative) in grey (white) regions; therefore, the nodal surface is located at the border between these two regions. Notice that the black dots belongs to the full nodal surface, but do not exhaust it.

The non-trivial aspect is that the nodal surface changes in the presence of interaction and may become very complicated, while the Pauli surface does not change, since it is determined only by symmetry. On the continuum, a straightforward implementation of the projection technique is given by the so-called *diffusion Monte Carlo*, in which the Schrödinger equation (in imaginary time) is solved by using a random sample of the wave function (e.g., walkers) that undergoes diffusion and branching processes, generated by the kinetic and potential terms of the Hamiltonian (Kalos et al., 1974; Ceperley and Alder, 1980; Foulkes et al., 2001). However, without any further constraint, walkers may diffuse in the whole phase space (corresponding to a "bosonic" state) and the "fermionic" character is hidden in the extremely small disproportion between walkers in positive and negative regions; this fact leads to insurmountable difficulties when performing simulations with a large number of electrons. In principle, we could solve the

https://doi.org/10.1017/9781316417041.011 Published online by Cambridge University Press

problem by restricting the simulations to regions where the wave function has a fixed sign and then use the symmetrization procedure to generate the wave function in the rest of the space; the problem is that we do not know the exact location of the boundaries of this region.

On the lattice, the sign problem is also present but it is not strictly related to the presence of fermions, since, also in bosonic systems, the ground-state wave function may have non-trivial signs, due to a "frustrating" kinetic energy with positive hoppings on generic lattices. The main difference between the continuum and the lattice is that, in the former one, the imaginary-time propagation with the free-electron kinetic term can be associated to a pure diffusion process (Kalos et al., 1974; Ceperley and Alder, 1980; Foulkes et al., 2001), while this is not always true in the latter one. Another important difference is that on the lattice the nodal surface is not defined, since the allowed configurations span a *discrete* Hilbert space.

The *fixed-node* method has been developed to deal with stable Monte Carlo simulations, for both continuum (Anderson, 1975, 1976; Moskowitz et al., 1982; Reynolds et al., 1982) and lattice (ten Haaf et al., 1995) models. This approach can be generalized to the complex case, by the *fixed-phase* approximation (Ortiz et al., 1993). The fixed-node approximation is a simple way to avoid the sign problem. In the continuum, it consists in forbidding electron moves that change the sign of the guiding function. In practice, we consider a diffusion process determined by the kinetic energy with the additional boundary condition that prevents node crossings: walkers that cross the node in a given diffusion step $|x\rangle \rightarrow |x'\rangle$ (i.e., having $\Psi_G(x)\Psi_G(x') < 0$, where $\Psi_G(x)$ denotes the guiding function used within the importance sampling procedure to fix the nodal surface) are killed. Here, only walkers close to the nodal surface are involved in this process. The antisymmetry of the wave function is replaced by boundary conditions and the approximation is equivalent to solving the Schrödinger equation inside one nodal pocket. Then, the full solution is uniquely determined by the shape of the nodal surface (and the potential). The fixed-node method gives a variational bound to the exact ground-state energy, since it corresponds to the best possible wave function with the boundary conditions determined by the guiding function. On the lattice, any configuration can be directly connected (through the Hamiltonian) to other configurations with opposite signs and, therefore, the fixed-node approximation is not limited to walkers that are "close" to the nodes.

10.2 A Simple Example on the Continuum

In order to have a first idea on how the sign problem arises in the projection technique, we consider a very simple example of a single particle moving in a one-dimensional box with hard walls at its boundaries. The Hamiltonian is given by:

https://doi.org/10.1017/9781316417041.011 Published online by Cambridge University Press

$$\mathcal{H} = -\frac{1}{2}\frac{d^2}{dx^2} + V(x), \tag{10.19}$$

where $0 \leq x \leq L$ and the potential $V(x)$ is even under reflection symmetry $\mathcal{R}$ with respect to the center of the box $x_c = L/2$. All wave functions must vanish at $x = 0$ and $x = L$ and can be classified according to their parity. The actual ground state has no nodes and can be called "bosonic": it is positive for all configurations. Instead, the first excited state has one node at x_c and can be called "fermionic": here, the wave function has both positive and negative regions. In this sense, the symmetry properties associated to a permutation of two particles in a many-body state are translated into the transformations under reflection symmetry $\mathcal{R}$. The ground state is even under reflection, while the first excited state is odd, implying that regions with positive and negative signs must exist.

Let us define two operators P_+ and P_- that project over the subspace of even (symmetric) and odd (anti-symmetric) wave functions:

$$P_\pm \Psi(x) = \frac{1}{2}\left[\Psi(x) \pm \Psi(L-x)\right]. \tag{10.20}$$

In the following, we will define an algorithm that will allow to sample the first excited state $\Upsilon_1(x)$ with *odd* reflection symmetry around the center, i.e., $\Upsilon_1(L-x) = -\Upsilon_1(x)$. On the continuum, it is necessary to use an exponential form of the projector, given the presence of an unbounded spectrum:

$$\lim_{\tau\to\infty} e^{-\tau\mathcal{H}}|\Psi_0\rangle \propto |\Upsilon_0\rangle. \tag{10.21}$$

In this case, the Green's function (without importance sampling) for an imaginary time-evolution τ is given by (Anderson, 1976; Ceperley and Alder, 1980; Reynolds et al., 1982):

$$\mathcal{G}(x', x) = \langle x'|e^{-\tau\mathcal{H}}|x\rangle, \tag{10.22}$$

which can be evaluated by using a Trotter approximation for a small evolution $\Delta\tau$ (Trotter, 1959; Suzuki, 1976a,b):

$$\mathcal{G}(x', x) \approx \frac{1}{\sqrt{2\pi\,\Delta\tau}} \exp\left[-\frac{(x'-x)^2}{2\Delta\tau}\right] \times \exp\left[-\Delta\tau V(x)\right], \tag{10.23}$$

where the first term can be related to a diffusion process, while the second one is the responsible for the branching scheme (Foulkes et al., 2001). An algorithm implementing the above iteration is given by Eqs. (10.7) and (10.8), where:

$$p_{x',x} = \frac{1}{\sqrt{2\pi\,\Delta\tau}} \exp\left[-\frac{(x'-x)^2}{2\Delta\tau}\right], \tag{10.24}$$

$$b_x = \exp\left[-\Delta\tau V(x)\right]. \tag{10.25}$$

https://doi.org/10.1017/9781316417041.011 Published online by Cambridge University Press

The former one can be simulated by considering a simple Langevin process for the configuration of the walker (see Chapter 4):

$$x_{n+1} = x_n + \sqrt{\Delta\tau}\,\eta_n, \tag{10.26}$$

where η_n is a random number with a Gaussian distribution (with zero mean and unit variance). The latter one determines the evolution of the weight of the walker.

Let us now consider the simplest case with $V(x) = 0$. Then, the exact ground-state ("bosonic") and the first-excited ("fermionic") wave functions are given by:

$$\Upsilon_0(x) = \sqrt{\frac{2}{L}} \sin\left(\frac{\pi x}{L}\right), \tag{10.27}$$

$$\Upsilon_1(x) = \sqrt{\frac{2}{L}} \sin\left(\frac{2\pi x}{L}\right). \tag{10.28}$$

with energies $E_0 = \pi^2/(2L^2)$ and $E_1 = (2\pi)^2/(2L^2)$. By performing the Markov process of Eqs. (10.24) and (10.25) without any other constraint, the walker will diffuse into the whole region $0 \leq x \leq L$ and equilibrate to the "bosonic" ground state. In order to obtain the "fermionic" wave function, we must consider a restricted space of wave functions $\Psi_{\rm fn}(x)$ that vanish outside a given interval $0 \leq x \leq L_{\rm fn}$. Then, the full anti-symmetrized state is obtained by acting with the projector P_- on such a wave function, as shown in Fig. 10.2:

$$\Psi_{\rm as}(x) = P_- \Psi_{\rm fn}(x). \tag{10.29}$$

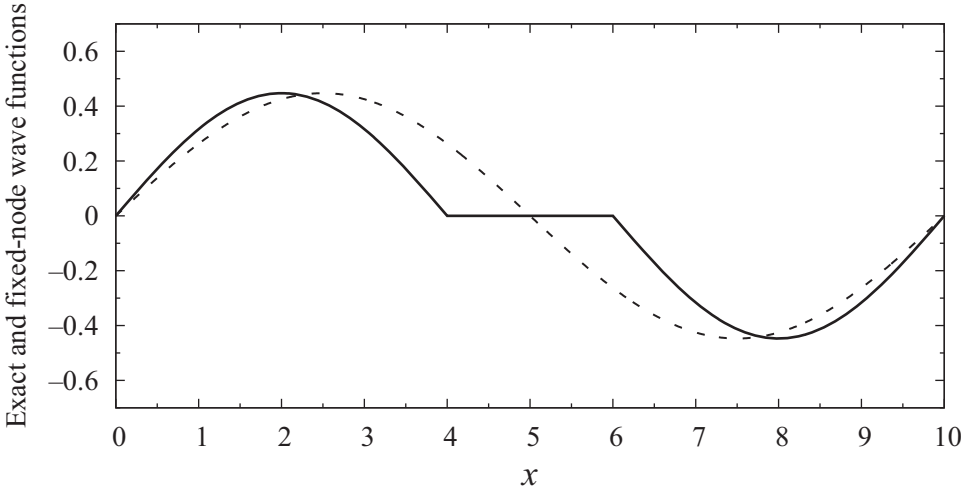

Figure 10.2 Wave functions for one particle in a box with $L = 10$ and $V(x) = 0$: the exact first-excited state (dashed line) with the node at $x = 5$ is compared with the fixed-node approximation (solid line) of it when the node is fixed at $x = 4$.

https://doi.org/10.1017/9781316417041.011 Published online by Cambridge University Press

In practice, we do not allow the walker to cross the barrier introduced with $L_{\rm fn}$. We can easily see that the extended wave function $\Psi_{\rm as}(x)$ has the same variational energy than $\Psi_{\rm fn}(x)$, which is restricted in the nodal pocket. Indeed, we have that:

$$E_{\rm fn} = \frac{\int_0^L dx\ \Psi_{\rm as}(x)\left(-\frac{1}{2}\frac{d^2}{dx^2}\right)\Psi_{\rm as}(x)}{\int_0^L dx\ \Psi_{\rm as}^2(x)} = \frac{\int_0^{L_{\rm fn}} dx\ \Psi_{\rm fn}(x)\left(-\frac{1}{2}\frac{d^2}{dx^2}\right)\Psi_{\rm fn}(x)}{\int_0^{L_{\rm fn}} dx\ \Psi_{\rm fn}^2(x)}. \tag{10.30}$$

It is important to emphasize that this equality holds despite the fact that the wave function has a discontinuous first derivative at the wrong nodal point (see Fig. 10.2), leading to:

$$\left.\frac{d^2\Psi_{\rm fn}(x)}{dx^2}\right|_{x=L_{fn}} = -\delta(x - L_{\rm fn})\Psi'_{\rm fn}(L_{\rm fn}), \tag{10.31}$$

where $\Psi'_{\rm fn}(L_{\rm fn}) = \lim_{x\to L_{\rm fn}^-} d\Psi_{\rm fn}(x)/dx$. In fact, the singular contribution coming from the delta-function does not play any role in the integrals, since the wave function vanishes at the nodal point $x = L_{\rm fn}$, and similarly for $x = L - L_{\rm fn}$.

Given the equality of Eq. (10.30), it is clear that the lowest possible energy can be obtained by optimizing the wave function just in the nodal pocket, which becomes a "bosonic" (i.e., node-less) problem that is suitable for the diffusion Monte Carlo approach. Notice that, in this simple case, we can also provide the analytical form of the best wave function, which is given by:

$$\Psi_{\rm fn}(x) = \sqrt{\frac{2}{L}}\sin\left(\frac{\pi x}{L_{\rm fn}}\right). \tag{10.32}$$

The corresponding energy is $E_{\rm fn} = \pi^2/(2L_{\rm fn}) \geq E_1$.

In general, we would like to emphasize the most important properties of the fixed-node approximation:

- The method is variational, as the projected wave function $\Psi_{\rm as}(x)$ has exactly the energy that is obtained with a "bosonic" ground-state calculation within a single nodal region.
- The fixed-node energy is very sensitive to the accuracy of the nodal surface of the wave function. In the previous example, the systematic error is linear in $\epsilon = L/2 - L_{\rm fn}$. Therefore, it is important to obtain a good description of the nodal surface (e.g., by a suitable optimization of the variational wave function).
- Although the energy corresponding to the projected wave function $\Psi_{\rm as}(x)$ and the one defined in the nodal pocket $\Psi_{\rm fn}(x)$ coincide, the same does not hold for the variance. For example, it is simple to show that the variance of the fixed-node ground state (10.32) is zero in the nodal pocket, but when the physical wave

https://doi.org/10.1017/9781316417041.011 Published online by Cambridge University Press

function is considered in the whole space $0 \leq x \leq L$, an infinite contribution to the variance comes from the delta-functions of Eq. (10.31). In this case, the infinite terms involving the square of delta-functions cancel only when the position of the node is exact.

In the previous example, the sign problem mainly arises because the Schrödinger equation (in imaginary time) is interpreted as a diffusion equation, whose steady state at large times is "bosonic," namely it is positive everywhere. This is the absolute ground state of any Hamiltonian with positive definite kinetic term and diagonal potentials. Instead, "fermionic" states can be seen as excited states of the same Hamiltonian, whenever the statistics of the particles is not specified *a priori* (in the spirit of the first-quantization formalism). The difficulty in this kind of calculation is embodied in the fact that we must extract the "fermionic" character of the observables from a small signal and a large noise, see Eq. (10.18). The previous example for the single particle in the box enlightens this issue.

10.3 A Simple Example on the Lattice

On the lattice, we are used to work in the second-quantization formalism, where the statistics of the particles is fully specified. Therefore, in this case, the diffusion process does not generically converge to the "bosonic" ground state, as in the continuum. However, whenever the kinetic terms have some negative signs, a sign problem is present. The simplest case is given by the lattice version of the previous example. Let us consider a single spinless particle on a one-dimensional lattice with L sites and open-boundary conditions, described by:

$$\mathcal{H} = -t_1 \sum_{i=1}^{L-1} c_i^\dagger c_{i+1} + \text{h.c.} - t_2 \sum_{i=1}^{L-2} c_i^\dagger c_{i+2} + \text{h.c.}, \tag{10.33}$$

where $c_i^\dagger$ (c_i) creates (destroys) the particle on the site i; t_1 and t_2 are the hopping amplitudes for nearest- and next-nearest-neighbor hoppings. The energy scale can be set by taking $t_1 = 1$. In the following, we will work in the local basis, where the states of the Hilbert space are specified by the position of the particle, i.e., $|i\rangle = c_i^\dagger |0\rangle$.

For $t_2 \geq 0$, the Hamiltonian has non-negative matrix elements and, therefore, can be sampled without sign problem by using the Green's function Monte Carlo. In this case a fully positive guiding function can be taken. Instead, for $t_2 < 0$, the Hamiltonian has both positive and negative elements and the sign problem is present. In particular, this happens even when the ground state is positive for all configurations (i.e., for small values of $|t_2|$). Therefore, on the lattice, the sign problem may exist even when the ground state is positive definite. Moreover, we

https://doi.org/10.1017/9781316417041.011 Published online by Cambridge University Press

emphasize that the sign problem on the lattice is not related to configurations that are close to the nodal surface but involves essentially all the configurations in the Hilbert space. For example, for the Hamiltonian of Eq. (10.33), all configurations have "frustrating" matrix elements with $\mathcal{H}_{x,x'} > 0$ when $t_2 < 0$. Finally, the sign problem is not related to the statistics of the particles (in this example, there is just one particle). Therefore, also bosonic models may have a sign problem, e.g., in presence of hopping terms that have the wrong sign.

On the lattice, the fixed-node approximation can be reformulated in terms of an effective Hamiltonian, which has all non-positive off-diagonal elements, such that a stable projection technique is possible (either by using the Green's function or reptation Monte Carlo approaches). Moreover, the calculations are kept under control, since a variational bound exists for the fixed-node energy.

10.4 The Fixed-Node Approximation on the Lattice

In this section, we present the fixed-node approximation on the lattice, as introduced by ten Haaf et al. (1995) and developed by Sorella (2002). This technique allows a refinement of a given guiding (variational) wave function $\Psi_G(x)$ by improving its amplitudes in a stable and controllable way (i.e., by lowering the energy with a reasonable computational effort). Before discussing the fixed-node approximation, it is useful to introduce a scheme that allows us to obtain the guiding function $\Psi_G(x)$ as the ground state of an effective Hamiltonian. For a given state, there are infinite "parent" Hamiltonians; here, we want to focus on the ones that are as close as possible to the original model and, most importantly, can be treated within stable Monte Carlo approaches. i.e., they have non-positive off-diagonal elements. Therefore, we consider the following family of effective (i.e., "variational") Hamiltonians:

$$\mathcal{H}^{\mathrm{var},\gamma}_{x,x'} = \begin{cases} \mathcal{H}_{x,x} + (1+\gamma)\mathcal{V}_{\mathrm{sf}}(x) - e_L(x) & \text{for } x' = x, \\ \mathcal{H}_{x,x'} & \text{for } x' \neq x,\ s_{x,x'} < 0, \\ -\gamma \mathcal{H}_{x,x'} & \text{for } x' \neq x,\ s_{x,x'} > 0, \end{cases} \tag{10.34}$$

where $\gamma \geq 0$ is a real parameter, $e_L(x)$ is the local energy of the guiding function:

$$e_L(x) = \sum_{x'} \mathcal{H}_{x,x'} \frac{\Psi_G(x')}{\Psi_G(x)}, \tag{10.35}$$

and the off-diagonal elements of the effective Hamiltonian are modified with respect to the original ones, according to their signs (including the ones of the guiding function):

$$s_{x,x'} = \Psi_G(x)\mathcal{H}_{x,x'}\Psi_G(x'). \tag{10.36}$$

https://doi.org/10.1017/9781316417041.011 Published online by Cambridge University Press

Finally, $\mathcal{V}_{\rm sf}(x)$ is a local potential that includes all the off-diagonal matrix elements generating sign problem, i.e., the ones with $s_{x,x'} > 0$:

$$\mathcal{V}_{\rm sf}(x) = \sum_{x':s_{x,x'}>0} \mathcal{H}_{x,x'} \frac{\Psi_G(x')}{\Psi_G(x)}. \tag{10.37}$$

Within this construction, the guiding function is an eigenstate of $\mathcal{H}^{{\rm var},\gamma}$ with zero eigenvalue, as can be verified by direct inspection; most importantly, for $\gamma \geq 0$, it is the unique ground state. Indeed, the unitary transformation $|x\rangle \to {\rm Sign}\Psi_G(x)|x\rangle$ changes all the off-diagonal matrix elements into non-positive ones. Therefore, by applying the Perron-Frobenius theorem (Meyer, 2000) (or, equivalently, by replicating the steps of section 3.8), we can show that $\Psi_G(x)$ is the non-degenerate ground state of the effective Hamiltonian (10.34). In other words, once including the importance sampling with $\Psi_G(x)$, the effective Hamiltonian has no sign problem, since $\mathcal{G}^{{\rm var},\gamma}_{x',x} = -\Psi_G(x')\mathcal{H}^{{\rm var},\gamma}_{x',x}/\Psi_G(x)$ is non-negative for $x' \neq x$. Hence, the standard Green's function Monte Carlo technique can be used to sample configurations corresponding to $\Psi^2_G(x)$. Then, an estimation of the variational energy E_G can be obtained by averaging the local energy $e_L(x)$. Notice that the diagonal term of the effective Hamiltonian can be arbitrarily large, due to the presence of the sign-flip potential (10.37); therefore, the continuous-time approach of section 8.4 is needed to have stable simulations.

We are now in the position to improve the variational description of the ground state of $\mathcal{H}$ and define a fixed-node scheme that is built from a slightly different effective Hamiltonian. Indeed, there are many configurations with a local energy that is below its average value and these configurations are likely to be energetically favorable in the true ground state. From this intuitive argument, we can expect to gain some energy by adding a diagonal potential term, which favors configurations that have a local energy below its average value, thus increasing the corresponding amplitudes. More precisely, from the variational Hamiltonian $\mathcal{H}^{{\rm var},\gamma}$, it is possible to define the fixed-node approximation on the lattice by adding a term that is linear in the local energy, with the purpose to improve the amplitudes of the variational *Ansatz*:

$$\mathcal{H}^{{\rm fn},\gamma}_{x,x'} = \mathcal{H}^{{\rm var},\gamma}_{x,x'} + \delta_{x,x'} e_L(x). \tag{10.38}$$

Again, for $\gamma \geq 0$, this Hamiltonian has non-positive off-diagonal elements (once importance sampling is included) and its ground state can be sampled by using projection techniques. The ground state of $\mathcal{H}^{{\rm fn},\gamma}$ has the same signs of $\Psi_G(x)$, thus justifying the name of "fixed-node" approximation, and has a lower energy than the variational one. Indeed, we can easily verify that:

$$\mathcal{H}^{{\rm fn},\gamma}|\Psi_G\rangle = \mathcal{H}|\Psi_G\rangle, \tag{10.39}$$

https://doi.org/10.1017/9781316417041.011 Published online by Cambridge University Press

which immediately implies that the expectation value of the fixed-node Hamiltonian over the guiding function is equal to the variational energy E_G:

$$\frac{\langle \Psi_G | \mathcal{H}^{\mathrm{fn},\gamma} | \Psi_G \rangle}{\langle \Psi_G | \Psi_G \rangle} = \frac{\langle \Psi_G | \mathcal{H} | \Psi_G \rangle}{\langle \Psi_G | \Psi_G \rangle} = E_G. \tag{10.40}$$

Therefore, the ground-state energy $E^{\mathrm{fn},\gamma}$ of the fixed-node Hamiltonian is certainly lower than (or at most equal to) the variational energy E_G. In order to prove that $E^{\mathrm{fn},\gamma}$ gives an upper bound of the true ground-state energy E_0 of $\mathcal{H}$, we re-write the fixed-node Hamiltonian in a compact way:

$$\mathcal{H}^{\mathrm{fn},\gamma} = \mathcal{H} + (1+\gamma)\mathcal{O}^{\mathrm{fn}}, \tag{10.41}$$

where $\mathcal{O}^{\mathrm{fn}}$ is defined in terms of the guiding function:

$$\mathcal{O}^{\mathrm{fn}}_{x,x'} = \begin{cases} \sum_{y: s_{x,y}>0} \frac{s_{x,y}}{\Psi_G^2(x)} & \text{for } x' = x, \\ -\mathcal{H}_{x,x'} & \text{for } x' \neq x \text{ and } s_{x,x'} > 0. \end{cases} \tag{10.42}$$

This operator is semi-positive definite. In fact, for any (real) state $|\Phi\rangle$, we have that:

$$\langle \Phi | \mathcal{O}^{\mathrm{fn}} | \Phi \rangle = \sum_{x,x': s_{x,x'}>0} s_{x,x'} \frac{\Phi^2(x)}{\Psi_G^2(x)} - \sum_{x,x': s_{x,x'}>0} s_{x,x'} \frac{\Phi(x)\Phi(x')}{\Psi_G(x)\Psi_G(x')}, \tag{10.43}$$

where, the first (second) term comes from the diagonal (off-diagonal) matrix elements the operator $\mathcal{O}^{\mathrm{fn}}$, respectively. By using the fact that $s_{x,x'}$ is symmetric, we can interchange the dummy variables x and x' in the first term and obtain:

$$\langle \Phi | \mathcal{O}^{\mathrm{fn}} | \Phi \rangle = \frac{1}{2} \sum_{x,x': s_{x,x'}>0} s_{x,x'} \left[\frac{\Phi(x)}{\Psi_G(x)} - \frac{\Phi(x')}{\Psi_G(x')} \right]^2 \geq 0. \tag{10.44}$$

Therefore, denoting the ground state of the fixed-node Hamiltonian by $|\Upsilon^{\mathrm{fn},\gamma}\rangle$, we have that:

$$E_0 \leq \frac{\langle \Upsilon^{\mathrm{fn},\gamma} | \mathcal{H} | \Upsilon^{\mathrm{fn},\gamma} \rangle}{\langle \Upsilon^{\mathrm{fn},\gamma} | \Upsilon^{\mathrm{fn},\gamma} \rangle} = \frac{\left\langle \Upsilon^{\mathrm{fn},\gamma} | [\mathcal{H}^{\mathrm{fn},\gamma} - (1+\gamma)\mathcal{O}^{\mathrm{fn}}] | \Upsilon^{\mathrm{fn},\gamma} \right\rangle}{\langle \Upsilon^{\mathrm{fn},\gamma} | \Upsilon^{\mathrm{fn},\gamma} \rangle} \leq E^{\mathrm{fn},\gamma}, \tag{10.45}$$

where we have used that $\mathcal{H}^{\mathrm{fn},\gamma} | \Upsilon^{\mathrm{fn},\gamma} \rangle = E^{\mathrm{fn},\gamma} | \Upsilon^{\mathrm{fn},\gamma} \rangle$ and the fact that the operator $\mathcal{O}^{\mathrm{fn}}$ is semi-positive definite. This result concludes the proof that $E^{\mathrm{fn},\gamma}$ improves the variational estimate: the fixed-node energy is lower than (or at most equal to) the variational estimate E_G and higher than (or at most equal to) the exact one:

$$E_0 \leq E^{\mathrm{fn},\gamma} \leq E_G. \tag{10.46}$$

https://doi.org/10.1017/9781316417041.011 Published online by Cambridge University Press

We would like to emphasize that the minimum energy (that can be computed without sign problem) is obtained for $\gamma = 0$. Indeed, by exploiting the Hellmann-Feynman theorem and Eq. (10.41), we have that:

$$\frac{dE^{\mathrm{fn},\gamma}}{d\gamma} = \frac{\langle \Upsilon^{\mathrm{fn},\gamma} | \mathcal{O}^{\mathrm{fn}} | \Upsilon^{\mathrm{fn},\gamma} \rangle}{\langle \Upsilon^{\mathrm{fn},\gamma} | \Upsilon^{\mathrm{fn},\gamma} \rangle} \geq 0, \tag{10.47}$$

which implies that $E^{\mathrm{fn},\gamma}$ is a monotonically increasing function of γ.

Moreover, it is worth mentioning that, within the projection technique, we get $E^{\mathrm{fn},\gamma}$ and not the expectation value of the original Hamiltonian over the fixed-node state, which is given by:

$$E_{\mathrm{ev}}^{\mathrm{fn},\gamma} = \frac{\langle \Upsilon^{\mathrm{fn},\gamma} | \mathcal{H} | \Upsilon^{\mathrm{fn},\gamma} \rangle}{\langle \Upsilon^{\mathrm{fn},\gamma} | \Upsilon^{\mathrm{fn},\gamma} \rangle}. \tag{10.48}$$

This quantity can be estimated by using Eq. (10.47):

$$E_{\mathrm{ev}}^{\mathrm{fn},\gamma} = E^{\mathrm{fn},\gamma} - (1+\gamma)\frac{dE^{\mathrm{fn},\gamma}}{d\gamma}. \tag{10.49}$$

Notice that, by performing several calculations at different values of $\gamma \geq 0$, we could in principle extrapolate $E^{\mathrm{fn},\gamma}$ to $\gamma = -1$ and obtain the exact ground-state energy. However, in the general case, such extrapolation is not easy to perform.

An important remark is that, on the lattice case, $E^{\mathrm{fn},\gamma}$ not necessarily gives the lowest energy that is compatible with the nodes of the guiding function. In fact, for the ground state of the fixed-node Hamiltonian $|\Upsilon^{\mathrm{fn},\gamma}\rangle$, the error is given by:

$$\Delta E = \left\langle \Upsilon^{\mathrm{fn},\gamma} | (\mathcal{H}^{\mathrm{fn},\gamma} - \mathcal{H}) | \Upsilon^{\mathrm{fn},\gamma} \right\rangle = (1+\gamma) \left\langle \Upsilon^{\mathrm{fn},\gamma} | \mathcal{O}^{\mathrm{fn}} | \Upsilon^{\mathrm{fn},\gamma} \right\rangle, \tag{10.50}$$

which is vanishing only if each individual term in the summation (10.44) vanishes. Therefore, having a guiding function with the correct signs is not sufficient to obtain the exact ground state. Instead, it is necessary that for *all* sign-flip pairs with $s_{x,x'} > 0$:

$$\frac{\Psi_G(x')}{\Psi_G(x)} = \frac{\Upsilon^{\mathrm{fn},\gamma}(x')}{\Upsilon^{\mathrm{fn},\gamma}(x)}. \tag{10.51}$$

Indeed, if this relation is verified, $|\Upsilon^{\mathrm{fn},\gamma}\rangle$ is a simultaneous eigenstate of $\mathcal{O}^{\mathrm{fn}}$ (with vanishing eigenvalue) and $\mathcal{H}^{\mathrm{fn},\gamma}$ and, therefore, it must be also an exact eigenstate of the original Hamiltonian, as $\mathcal{H} = \mathcal{H}^{\mathrm{fn},\gamma} - (1+\gamma)\mathcal{O}^{\mathrm{fn}}$. This is an important difference with respect to the fixed-node approach on the continuum, where it is only the sign of the guiding function that matters (if the nodes are correctly placed, the exact result is obtained). By contrast, on the lattice, the sign and the relative amplitudes of the wave function in configurations that are connected by a sign flip must be correct. For example, in Fig. 10.3, we report the results for the model (10.33) on 30 sites, with $t_2 = -0.2$ and -0.4. In the former case, the true ground state is positive everywhere, but the fixed-node approach is not exact when taking a positive guiding

https://doi.org/10.1017/9781316417041.011 Published online by Cambridge University Press

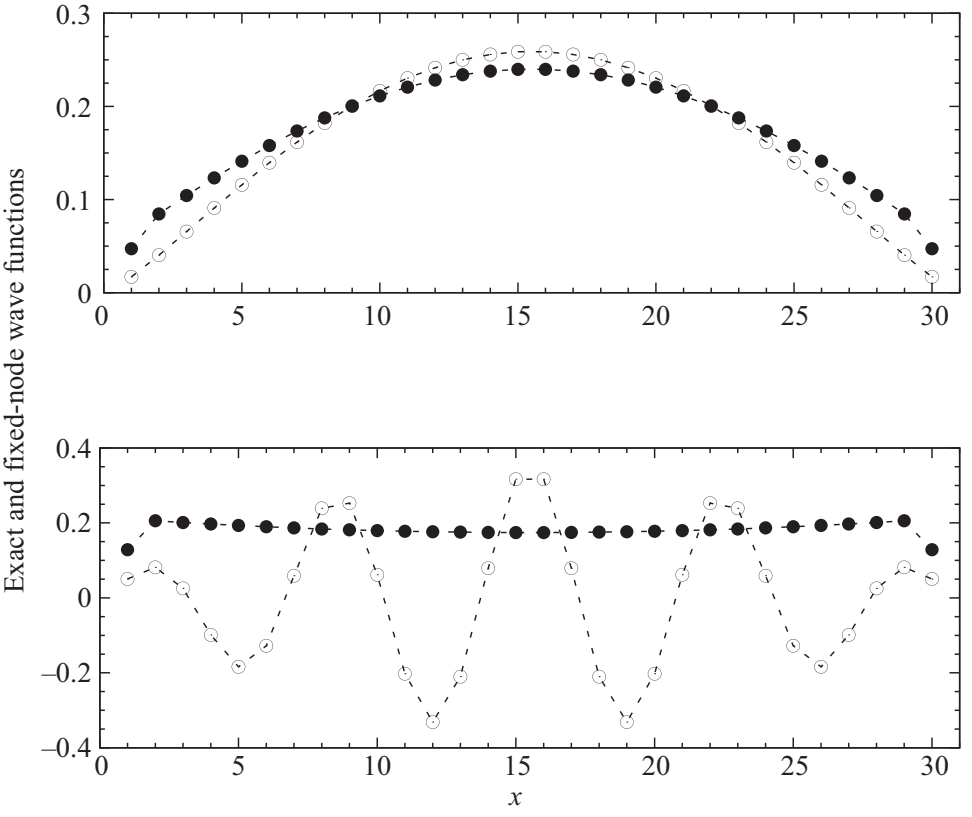

Figure 10.3 Comparison between the exact (empty circles) and the fixed-node (full circles) wave functions for the ground state of the Hamiltonian of Eq. (10.33) for the cases with $t_2 = -0.2$ (upper panel) and $t_2 = -0.4$ (lower panel); the number of sites is $L = 30$. The guiding function is taken to be constant, e.g., $\Psi_G(x) = 1/\sqrt{L}$.

function, e.g., $\Psi_G(x) = 1/\sqrt{L}$; indeed, we get $E^{\mathrm{fn},0}/t_1 = -1.59196$, to be compared with $E_0/t_1 = -1.59775$. The situation is much worse when also the true ground state is not positive definite, i.e., for $t_2 = -0.4$; here, still using the same guiding function as before, we get $E^{\mathrm{fn},0}/t_1 = -1.20192$, while the true ground-state energy is $E_0/t_1 = -1.41588$.

10.5 Practical Implementation

The fixed-node approximation can be applied to the Green's function and Reptation Monte Carlo techniques. The practical implementation follows the ones described in Chapters 8 and 9 with the only difference that all the new configurations are selected by considering the fixed-node Hamiltonian defined by Eqs. (10.34) and (10.38) instead of the original one.

https://doi.org/10.1017/9781316417041.011 Published online by Cambridge University Press